

# Global dynamics of radiatively inefficient accretion flows: advection versus convection

Ju-Fu Lu <sup>\*</sup>, Shuang-Liang Li and Wei-Min Gu

*Department of Physics, Xiamen University, Xiamen 361005, China*

## ABSTRACT

We obtain global solutions of radiatively inefficient accretion flows around black holes. Whether and where convection develops in a flow are self-consistently determined with the mixing-length theory. The solutions can be divided into three types according to the strength of normal viscosity. Type I solution corresponds to large viscosity parameter  $\alpha \gtrsim 0.1$ , which is purely advection-dominated and with no convection, and has been extensively studied in the literature. Type II solution is for moderate  $\alpha \sim 0.01$ , which has a three-zone structure. The inner zone is advection-dominated, the middle zone is convection-dominated and ranges from a few tens to a few thousands of gravitational radii, and the outer zone is convectively stable and matches outward a Keplerian disc. The net energy flux throughout the flow is inward as in type I solution. Type III solution which is for small  $\alpha \lesssim 0.001$  consists of two zones as Abramowicz et al. suggested previously: an inner advection-dominated zone and an outer convection-dominated zone, separated at a radius of a few tens of gravitational radii. This type of solution has an outward net energy flux. In both type II and III solutions the radial density profile is between the 1/2 law of self-similar convection-dominated accretion flow model and the 3/2 law of self-similar advection-dominated accretion flow model, and the efficiency of energy release is found to be extremely low. Our results are in good agreement with those of recent numerical simulations.

**Key words:** accretion, accretion discs – black hole physics – convection – hydrodynamics

<sup>\*</sup> E-mail: lujf@xmu.edu.cn

## 1 INTRODUCTION

Accreting black holes in nearby galactic nuclei and low state X-ray binaries are much dimmer than the standard Shakura-Sunyaev disc model would predict. This phenomenon has been modeled within the framework of a radiatively inefficient accretion flow (RIAF). In such a flow, radiative losses are small because of the low particle density of the accreting plasma at low mass accretion rates. It was then suggested that most of the released gravitational and rotational energies of accreting plasma is advected inward in the form of the internal energy, and is finally absorbed by the black hole. Such a particular model of RIAFs was called the advection-dominated accretion flow (ADAF) and attracted a considerable attention during the last decade (see Narayan, Mahadevan & Quataret 1998 and Narayan 2002 for reviews).

At the same time when the ADAF model was proposed, it was realized that ADAFs are likely to be convectively unstable in the radial direction because of the inward increase of the entropy of accreting gas (Narayan & Yi 1994). Two dimensional (2D) and three dimensional (3D) hydrodynamical (HD) simulations of low viscosity RIAFs have confirmed the convective instability in these flows (Igumenshchev, Chen & Abramowicz 1996; Igumenshchev & Abramowicz 1999, 2000; Stone, Pringle & Begelman 1999; Igumenshchev, Abramowicz & Narayan 2000; McKinney & Gammie 2002). Narayan, Igumenshchev & Abramowicz (2000) and Quataert & Gruzinov (2000) constructed another analytical model of RIAFs, which was based on a self-similar solution and reproduced the basic features of the HD simulations, and was called the convection-dominated accretion flow (CDAF). The dynamical structure of CDAFs is characterized by a 1/2 law of the radial density profile,  $\rho \propto R^{-1/2}$ , shallower than that for the self-similar ADAF model,  $\rho \propto R^{-3/2}$ , where  $\rho$  is the density and  $R$  is the radius. In the limit of perfect self-similarity, CDAFs are nonaccreting with the radial velocity  $v = 0$  and the mass accretion rate  $\dot{M} = 0$  (Narayan et al. 2000). In realistic CDAFs  $\dot{M}$  is small but not exactly zero, leading to a finite  $v \propto R^{-3/2}$ . The low luminosities of RIAFs are referred to a small convective luminosity,  $L_c = \varepsilon \dot{M} c^2$ , with the convective efficiency  $\varepsilon \approx 0.01$  (Igumenshchev & Abramowicz 2001), rather than to the inward bulk advection of energies as in the ADAF model.

The self-similar CDAF model (as well as all other self-similar models), though very clear and instructive, has its limitations. It is only a local, not a global solution of a RIAF, in the sense that it can only be valid for the region of a RIAF far away from the boundaries. In particular, it cannot reflect the transonic radial motion – the most fundamental feature

of black hole accretion flows. Advection ought to be important in the vicinity of the black hole because of the large radial velocity of the accretion flow, so the inner region of RIAFs is likely to be better described by the ADAF model. Abramowicz et al. (2002) did suggest such a two zone structure of RIAFs: an outer convection-dominated zone and an inner advection-dominated zone, separated at a transition radius  $\sim 50R_g$  ( $R_g = 2GM/c^2$  is the gravitational radius, with  $M$  being the black hole mass).

In this paper we solve numerically the set of one dimensional (1D) height-integrated dynamical equations and obtain global solutions of RIAFs around nonrotating black holes. Such a global solution is more exact and complete than the self-similar solution on one hand, and is simpler and more transparent than the 2D or 3D simulations on the other hand. Remember that the ADAF model was also in a self-similar form when it was proposed (Narayan & Yi 1994, 1995), and was later checked and improved by authors working on the 1D global solution (e.g. Narayan, Kato & Honma 1997; Chen, Abramowicz & Lasota 1997; Lu, Gu & Yuan 1999).

## 2 EQUATIONS

We consider a set of stationary height-integrated equations describing a RIAF around a nonrotating black hole (e.g. Narayan et al. 2000; Abramowicz et al. 2002). In the absence of mass outflows, the continuity equation reads

$$\dot{M} = -2\pi R \Sigma v = \text{const}, \quad (1)$$

where  $\Sigma = 2H\rho$  is the surface density,  $H = c_s/\Omega_K$  is the scale height,  $c_s = (P/\rho)^{1/2}$  is the sound speed,  $P$  is the pressure,  $\Omega_K = (GM/R)^{1/2}/(R - R_g)$  is the Keplerian angular velocity in the well known Paczyński & Wiita (1980) potential.

The radial momentum equation is as usual

$$v \frac{dv}{dR} + (\Omega_K^2 - \Omega^2)R + \frac{1}{\rho} \frac{dP}{dR} = 0, \quad (2)$$

where  $\Omega$  is the angular velocity. Note that the ram-pressure term  $v dv/dR$  in equation (2) was ignored in the self-similar CDAF model (Narayan et al. 2000), while we include it here in order to have a global solution.

In the presence of convection, the angular momentum and energy equations can be written as

$$J = J_{adv} + J_{vis} + J_{con} = \text{const}, \quad (3)$$

and

$$F = F_{adv} + F_{dis} + F_{con} = \text{const}, \quad (4)$$

where  $J$ ,  $J_{adv}$ ,  $J_{vis}$  and  $J_{con}$  are the total, advective, viscous and convective angular momentum flux, and  $F$ ,  $F_{adv}$ ,  $F_{dis}$  and  $F_{con}$  are the total, advective, dissipative and convective energy flux, respectively. In the angular momentum equation (3), advection moves angular momentum inward ( $v < 0$ ),

$$J_{adv} = 2\pi R \Sigma v (\Omega R^2).$$

Normal viscosity transports angular momentum outward, i.e. the viscous angular momentum flux is oriented down the angular velocity gradient,

$$J_{vis} = -2\pi R \nu \Sigma R^2 (d\Omega/dR),$$

where  $\nu$  is the kinematic viscosity coefficient,  $\nu = \alpha c_s^2 / \Omega_K$ , with  $\alpha$  being the constant Shakura-Sunyaev parameter. The basic question of how convection transports angular momentum is a complex topic. As discussed by Igumenshchev (2002), in magnetohydrodynamical (MHD) CDAFs convection can transport angular momentum either inward or outward, depending on the properties of turbulence in rotating magnetized plasma, which are not fully understood yet; but in HD CDAFs we consider here, convection transports angular momentum inward, i.e. the convective flux is directed down the specific angular momentum gradient,

$$J_{con} = -2\pi R \nu_{con} \Sigma [d(\Omega R^2)/dR],$$

where  $\nu_{con}$  is the diffusion coefficient. In the energy equation (4) the advective energy flux is

$$F_{adv} = 2\pi R \Sigma v B,$$

where  $B = 0.5v^2 - GM/(R - R_g) + 0.5R^2\Omega^2 + \gamma c_s^2/(\gamma - 1)$  is the Bernoulli function, with  $\gamma$  being the adiabatic index. The dissipative energy flux is due to both the viscous and the convective shear stress,

$$F_{dis} = \Omega(J_{vis} + J_{con}).$$

The convective energy flux can be expressed in the form,

$$F_{con} = -2\pi R \nu_{con} \Sigma T (ds/dR),$$

where  $s$  is the specific entropy and  $T$  is the temperature, and  $T \frac{ds}{dR} \equiv \frac{1}{\gamma-1} \frac{dc_s^2}{dR} - \frac{c_s^2}{\rho} \frac{d\rho}{dR}$ .

The same  $\nu_{con}$  appears in both the expression for  $J_{con}$  and that for  $F_{con}$ . This means that

we have adopted the assumption of Narayan et al. (2000) that all transport phenomena due to convection have the same diffusion coefficient, which is defined as

$$\nu_{con} = (L_M^2/4)(-N_{eff}^2)^{1/2}, \quad (5)$$

where  $L_M = 2^{-1/4}l_M H_P$  is the characteristic mixing length,  $l_M$  is the dimensionless mixing-length parameter (taken to be equal to  $\sqrt{2}$  in our calculations),  $H_P = -dR/d\ln P$  is the pressure scale height, and  $N_{eff}$  is the effective frequency of convective blobs,

$$N_{eff}^2 = N^2 + \kappa^2, \quad (6)$$

with  $N$  and  $\kappa$  being the Brunt-Väisälä frequency and the epicyclic frequency, respectively,

$$N^2 = -\frac{1}{\rho} \frac{dP}{dR} \frac{d}{dR} \ln \left( \frac{P^{1/\gamma}}{\rho} \right),$$

and

$$\kappa^2 = 2\Omega^2 \frac{d\ln(\Omega R^2)}{d\ln R}.$$

Note that  $\kappa \neq \Omega$  in general,  $\kappa = \Omega$  only for the self-similar scaling  $\Omega \propto R^{-3/2}$  (Narayan et al. 2000). Convection is present whenever  $N_{eff}^2 < 0$ .  $\nu_{con}$  can also be written in the form similar to normal viscosity,

$$\nu_{con} = \alpha_{con} c_s^2 / \Omega_K, \quad (7)$$

where  $\alpha_{con}$  is a dimensionless parameter that describes the strength of convective diffusion, it is not a constant, whereas the Shakura-Sunyaev viscosity parameter  $\alpha$  is assumed to be.

The angular momentum equation (3) can be rewritten explicitly as

$$\frac{(\alpha + \alpha_{con})c_s^2 R^2}{\Omega_K v} \frac{d\Omega}{dR} = \Omega R^2 \left( 1 - \frac{2\alpha_{con}c_s^2}{R\Omega_K v} \right) - j, \quad (8)$$

where  $j$  is a constant. We impose a no-torque condition  $d\Omega/dR = 0$  at the inner boundary of the accretion flow, so  $j$  represents the specific angular momentum accreted by the black hole in the absence of convection (i.e. when  $\alpha_{con} = 0$ ). The differential form of the energy equation (4) is

$$\Sigma v T \frac{ds}{dR} = \frac{c_s^2}{\Omega_K} \Sigma R \left[ (\alpha + \alpha_{con}) R \left( \frac{d\Omega}{dR} \right)^2 + 2\alpha_{con}\Omega \frac{d\Omega}{dR} \right] + \frac{1}{R} \frac{d}{dR} \left( R \frac{\alpha_{con}c_s^2}{\Omega_K} \Sigma T \frac{ds}{dR} \right). \quad (9)$$

Equations (1), (2), (8) and (9) can be solved for four variables  $\rho$ ,  $v$ ,  $c_s$  and  $\Omega$  as functions of  $R$ , provided the constant flow parameters  $M$ ,  $\dot{M}$ ,  $\alpha$ ,  $\gamma$  and  $j$  are given. Note that  $\alpha_{con}$  is not another unknown quantity, it can be obtained self-consistently from equations (5) and (7) if  $N_{eff}^2$  calculated from equation (6) is negative (i.e. there is convection), otherwise it is zero (i.e. no convection).

### 3 GLOBAL SOLUTIONS

We use the standard Runge-Kutta method to solve the set of three differential equations (2), (8) and (9) for three unknowns  $v$ ,  $c_s$  and  $\Omega$ , and then obtain  $\rho$  from equation (1). We integrate the differential equations from the sonic point  $R_s$  (where  $|v| = c_s$ ) both inward and outward. As discussed in detail by Abramowicz et al. (2002),  $R_s$  is not an additional free parameter, it is an eigenvalue and is self-consistently determined in a regular transonic solution. At and inside  $R_s$  the flow ought to be advection-dominated, and convection is unimportant. So we set  $\alpha_{con} = 0$  in equations (8) and (9) when starting the integration from  $R_s$ . The inward, supersonic part of the solution extends to the inner boundary of the flow, i.e. to a radius where the no-torque condition  $d\Omega/dR = 0$  (i.e.  $\Omega R^2 = j$ ) is satisfied. More important for our purpose here is the outward, subsonic part of the solution. The Runge-Kutta method does not require any a priori outer boundary conditions, we just observe how the outward solution evolves with increasing  $R$  until a reasonable outer boundary is found. Whether and where there is convection in the flow are judged in the following self-consistent manner: at each radius we calculate  $N_{eff}^2$  from equation (6), if  $N_{eff}^2 \geq 0$ , i.e. no convection develops, then  $\alpha_{con}$  keeps to be zero; when  $N_{eff}^2 < 0$ , i.e. convection is present, we obtain a non-zero  $\alpha_{con}$  from equations (5) and (7), and put it into equations (8) and (9) for the next step of the outward integration.

We obtain three types of global solutions depending on the value of the viscosity parameter  $\alpha$ :

I. Pure ADAF solution for large  $\alpha \gtrsim 0.1$ . In this case viscous action is so strong that the flow is totally advection-dominated, and no convection develops at all. This type of solution has been extensively investigated in the literature (e.g. Narayan et al. 1997), and we do not repeat it here.

II. Three zone solution for moderate  $\alpha \sim 0.01$ . Fig. 1 provides an example of this type of solution, with  $\alpha = 0.01$ ,  $\gamma = 5/3$ ,  $j = 1.646(cR_g)$ , and  $R_s = 2.3R_g$ . Fig. 1(a) shows how the convective diffusion parameter  $\alpha_{con}$  varies with the radius  $R$ , from which a three-zone structure is clearly seen. In the middle zone ranging from  $R = 34R_g$  to  $R = 2300R_g$ , convection develops and plays a dominant role, in the sense that  $\alpha_{con} > \alpha$  for almost all the zone. For the inner zone ( $R < 34R_g$ ) and the outer zone ( $R > 2300R_g$ ) convection ceases to exist ( $\alpha_{con} = 0$ ). Fig. 1(b) draws the radial profile of the density  $\rho$  (the solid line). For comparison, the profiles  $\rho \propto R^{-3/2}$  of the self-similar ADAF solution (the dashed line) and

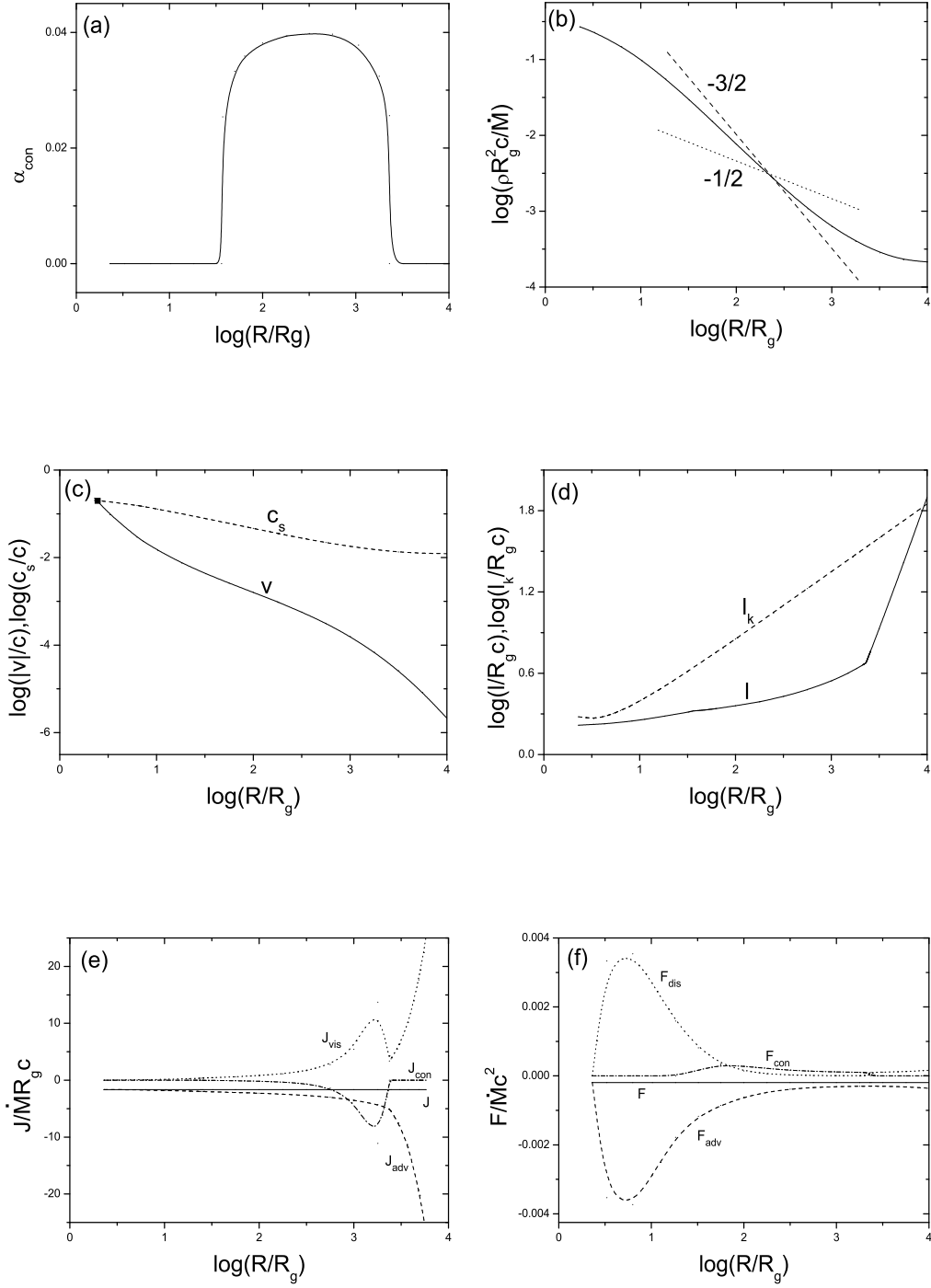


**Figure 1.** Example of type II three-zone solution for the viscosity parameter  $\alpha = 0.01$ . (a), (b), (c), (d), (e) and (f) are for the convective diffusion parameter  $\alpha_{con}$ ; the density  $\rho$ ; the radial velocity  $v$  and the sound speed  $c_s$ ; the specific angular momentum  $l$  and the Keplerian angular momentum  $l_K$ ; the total angular momentum flux  $J$  and its advective component  $J_{adv}$ , viscous component  $J_{vis}$  and convective component  $J_{con}$ ; and the total energy flux  $F$  and its advective component  $F_{adv}$ , dissipative component  $F_{dis}$  and convective component  $F_{con}$ ; respectively.

$\rho \propto R^{-1/2}$  of the self-similar CDAF solution (the dotted line) are also given. It is seen that the radial density distribution in the global solution is in between, i.e. shallower than that for the self-similar ADAF solution, and steeper than that for the self-similar CDAF solution. Fig. 1(c) is for the radial velocity  $v$  (the solid line) and the sound speed  $c_s$  (the dashed line). The sonic point is marked by a filled square. Fig. 1(d) is for the specific angular momentum  $l = \Omega R^2$  (the solid line) and the Keplerian angular momentum  $l_K = \Omega_K R^2$  (the dashed line). The profiles of  $l$  in the three zones are distinct from each other: in the inner zone  $l$  behaves as in the pure ADAF solution of type I; in the middle zone the profile is greatly flattened comparing with the pure ADAF solution would have, because of the strong inward transport of angular momentum by the convective flux; while in the outer zone  $l$  increases steeply with increasing  $R$ , and reaches the Keplerian value  $l_K$  at  $R = 9252R_g$ , and this radius can be reasonably regarded as the outer boundary of the flow. Fig. 1(e) is devoted to the angular momentum flux, in which the total flux  $J$ , the advective component  $J_{adv}$ , the viscous component  $J_{vis}$  and the convective component  $J_{con}$  are denoted by the solid, dashed, dotted and dot-dashed line, respectively. In the inner advection-dominated zone  $J_{con} = 0$ , and  $J_{vis}$  is very small, so  $J$  is dominated by  $J_{adv}$ . In the middle convection-dominated zone  $J_{con}$  (inward) and  $J_{vis}$  (outward) almost cancel each other, while  $J_{adv}$  is relatively small. In the outer no-convection zone  $J_{con}$  becomes zero again, and both  $J_{vis}$  and  $J_{adv}$  (its absolute value) increase with increasing  $R$ . The competition of these three components results in a constant net flux throughout the flow,  $J = -\dot{M}j = -1.646(\dot{M}cR_g)$ , which is inward. In Fig. 1(f) which is for the energy flux, the total flux  $F$ , the advective component  $F_{adv}$ , the dissipative component  $F_{dis}$  and the convective component  $F_{con}$  are denoted again by the solid, dashed, dotted and dot-dashed line, respectively. In the inner and the outer zone  $F_{con} = 0$ , and  $F_{adv}$  (inward) and  $F_{dis}$  (outward) almost balance in power. In the middle zone  $F_{dis}$  is small, and  $F_{adv}$  is nearly balanced by  $F_{con}$  (outward) instead. The net result of the competition is again a constant flux  $F = -0.00019(\dot{M}c^2)$ , with the efficiency  $\varepsilon = 0.00019$ . Note that although  $F_{con}$  alone is positive,  $F$  is negative, i.e. the released gravitational energy is dragged inward as in ADAFs, and that the efficiency of energy release is very small.

III. Two zone solution for small  $\alpha \lesssim 0.001$ . This type of solution has been suggested previously by Abramowicz et al. (2002), of which an example is given by Fig. 2, with  $\alpha = 0.001$ ,  $\gamma = 5/3$ ,  $j = 1.88(cR_g)$ , and  $R_s = 2.1R_g$ . The arrangements and the symbols of the figure are the same as for Fig. 1. The solution has a two-zone structure, i.e. an inner advection-

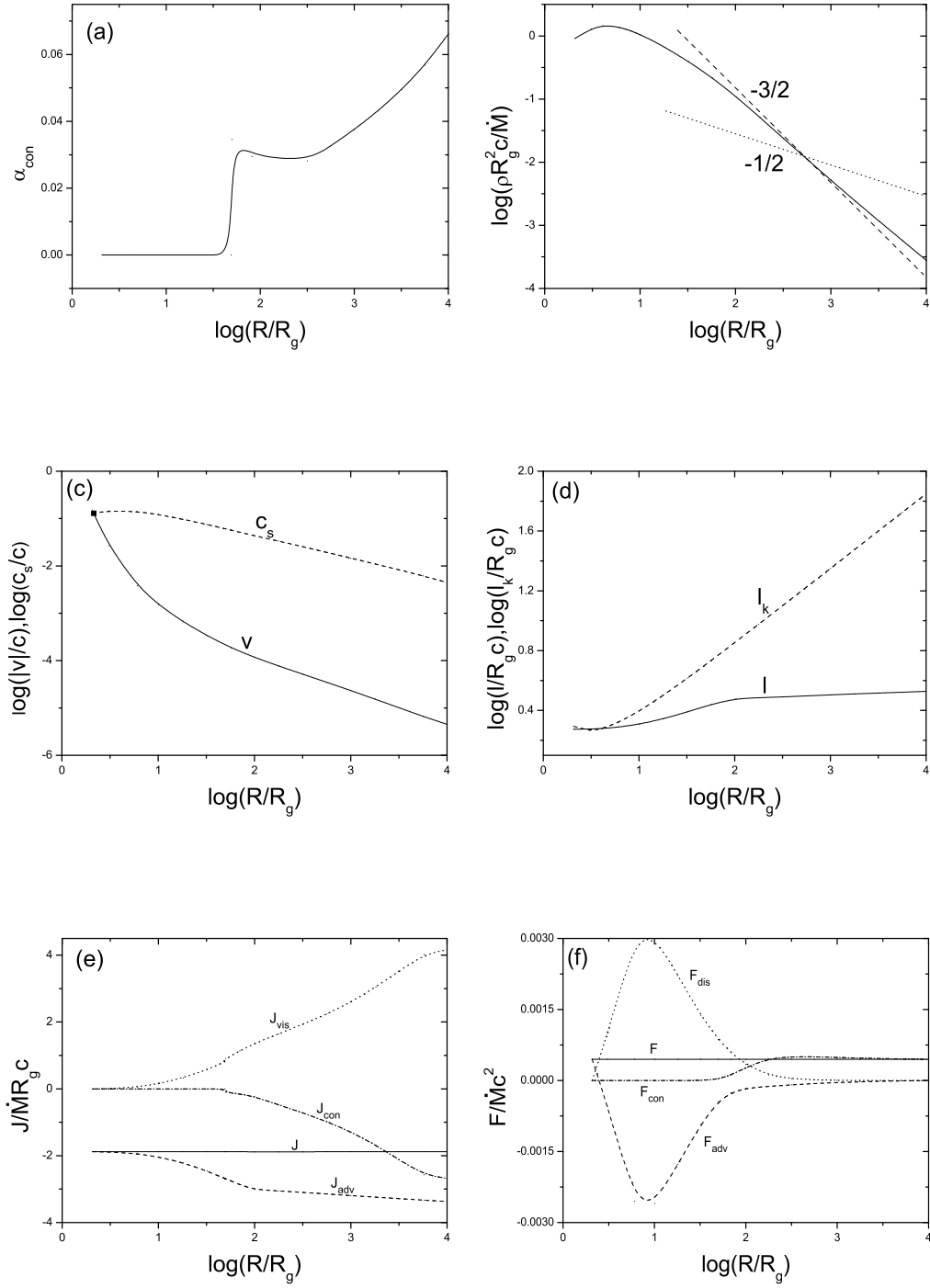


**Figure 2.** Example of type III two-zone solution for  $\alpha = 0.001$ . The arrangements are the same as for Fig. 1.

dominated zone and an outer convection-dominated zone, with a transition occurring at  $R = 49R_g$ . It is seen from Fig. 2(a) that  $\alpha_{con} = 0$  in the inner zone, it is non-zero and increases with increasing  $R$  in the outer zone, i.e. convection does not cease to exist for large radii as in type II solution. In Fig. 2(b) the radial density profile is also between the line of self-similar ADAF solution ( $\propto R^{-3/2}$ ) and that of self-similar CDAF solution ( $\propto R^{-1/2}$ ). In Fig. 2(c) the profile of  $v$  in the outer zone is shallower than that in Fig. 1(c), proving a stronger effect of convective motion against advection. The power of convection is most clearly seen from Fig. 2(d): in the outer zone the inward transport of angular momentum by convection is so effective that  $l$  keeps being almost constant. Accordingly, the combined inward flux of  $J_{con}$  and  $J_{adv}$  overcomes the outward flux  $J_{vis}$ , resulting in an inward net flux  $J = -1.88(\dot{M}cR_g)$ , as drawn in Fig. 2(e). Fig. 2(f) is noticeable, as it shows that in the outer zone both  $F_{adv}$  and  $F_{dis}$  tend to be zero for large radii, and the outward  $F_{con}$  really dominates, giving a net energy flux which is positive,  $F = 0.00045(\dot{M}c^2)$ , with  $\varepsilon = 0.00045$ . As Abramowicz et al. (2002) argued but not explicitly proved, the outward  $F$  is produced in the inner zone where most of the dissipatively released gravitational energy (i.e.  $F_{dis}$ ) is advected inward (i.e.  $F_{adv}$ ), with a small remainder that bubbles out through the flow. This outward  $F$  is a characteristic feature of this type of solution, qualitatively different from the case of ADAFs.

Figs. 1 and 2 are for  $\gamma = 5/3$ . We have also made calculations for different values of  $\gamma$  ( $4/3 \leq \gamma \leq 5/3$ ), and the results obtained remain qualitatively similar.

## 4 DISCUSSION

We have shown that global solutions of black hole RIAFs can be divided into three types according to the strength of normal viscosity. When viscosity is strong (large  $\alpha$ ), convection plays no role, and the flow is totally advection-dominated (type I solution). If viscosity is moderate (smaller  $\alpha$ ), the flow has a three-zone structure, and convection is important only in the middle zone which ranges from a few tens to a few thousands of  $R_g$ ; the net energy flux is still inward as in ADAFs (type II solution). In the case of weak viscosity (very small  $\alpha$ ), the flow consists of two zones with a transition radius of a few tens of  $R_g$ , and convection dominates in the outer zone; the net energy flux becomes outward (type III solution). Our type III solution confirms the idea of two-zone structure proposed by Abramowicz et al. (2002), though the transition radius is defined in somewhat different ways.

Our results are in good agreement with those of numerical simulations, and may be somewhat detailed improvements on the self-similar CDAF model. Here we address a few points:

1. As Igumenshchev & Abramowicz (2001) summarized, 2D HD simulations of RIAFs had proven that for  $\alpha \lesssim 0.03$  and all the reasonable values of  $\gamma$  the flow is convectively unstable, which agrees very well with our results here; and that convection transports angular momentum inward and no outflows are present, which support our assumptions of inward flux  $J_{con}$  and constant accretion rate  $\dot{M}$ .
2. In the self-similar CDAF model convection was assumed a priori to present throughout the flow, and the convective diffusion parameter  $\alpha_{con}$  was treated as a constant (Narayan et al. 2000); while in our global solutions whether and where convection develops in a given flow are self-consistently determined by calculating the effective frequency  $N_{eff}$  at each radius, and  $\alpha_{con}$  is a function of  $R$  and is also calculated.
3. In our solutions the density profile is between the 1/2 law of self-similar CDAF solution and 3/2 law of self-similar ADAF solution. We think this is reasonable, because the self-similar CDAF and ADAF solutions should be regarded as two ideal extremes, and should be modified under the influence of boundary conditions in global solutions. In their most recent 3D MHD simulations of RIAFs, Pen, Matzner & Wong (2003) found a quasi-hydrostatic density profile  $\rho \propto R^{-0.72}$  (i.e. also between the 1/2 and 3/2 laws).
4. As Pen et al. (2003) pointed out, the 1/2 law derives from assuming a positive convective energy flux  $F_{con}$ . In our solutions although  $F_{con} > 0$  holds, the total energy flux  $F$  can be either positive (type III solution) or negative (type II solution), depending on whether convection really dominates. In fact Pen et al. (2003) also obtained  $F < 0$ , which is consistent with our type II solution.
5. The efficiency of energy release of RIAFs was estimated previously as  $\varepsilon \approx 0.003 - 0.01$  (e.g. Igumenshchev & Abramowicz 2000; Abramowicz et al. 2002), while in our solutions  $\varepsilon$  is significantly smaller (it is 0.00019 in Fig. 1 and 0.00045 in Fig. 2). This is probably because those authors referred  $\varepsilon$  only to the convective energy flux  $F_{con}$  (they named  $\varepsilon$  'convective efficiency'), while we refer it to the total energy flux  $F$ . The extremely low efficiency in our solutions might have observational implications, e.g. it might help explain the immense discrepancy between the dynamically estimated mass accretion rate and the observed luminosity in the Galactic center and other nearby galaxies (e.g. Pen et al. 2003).

Concerning these main results, there are also several points we need to comment on, only

very briefly:

1. Our treatment of convection here is appropriate for viscous HD flows and not necessarily for MHD ones. Although since the work of Balbus & Hawley (1991) it has become widely agreed that the magneto-rotational instability is the detailed mechanism that produces viscosity, it is not yet clear how the MHD approach could change the results of the HD model. For example, depending on the assumed topology of the magnetic field in the flow, some studies find quite good agreement between numerical MHD simulations and analytical works on HD CDAFs (e.g. Machida, Matsumoto & Mineshige 2001); others, however, claim that there are significant differences (e.g. Hawley & Balbus 2002). It is therefore not surprising that we compare our results here with not only HD, but also some MHD simulations.
2. We identify 5 controlling parameters of the flow, namely  $M$ ,  $\dot{M}$ ,  $\alpha$ ,  $\gamma$  and  $j$ , from which the detailed flow structure is determined. Of these parameters,  $M$ ,  $\dot{M}$  and  $j$  scale variables  $R$ ,  $\rho$ ,  $l$ ,  $J$  and  $F$ , then our numerical calculations show that  $\alpha$  is the only important one in determining the solution topology, and  $\gamma$  seems to be insignificant. These results are consistent with those of previous 2D HD simulations. For example, Fig. 1 of Igumenshchev & Abramowicz (2001) shows clearly that for small  $\alpha \lesssim 0.03$ , flows are convectively unstable regardless of the value of  $\gamma$ ; this agrees well with our type II and III solutions. However, the same figure also indicates that in the case of large  $\alpha \gtrsim 0.1$ ,  $\gamma$  is important in determining other properties of flows such as large-scale circulations and outflows; this would complicate our type I solution, but has gone beyond the scope of the present paper.
3. We use  $N_{eff}^2 < 0$  for the onset of convection. One might wonder if this is a sufficient criterion. Of course the best way of verification is numerical simulations. Another simpler means is to estimate the Rayleigh number defined as  $R_a = ga\Delta T R^3/\nu^2$ , taking the thermal diffusivity to equal the kinematic viscosity  $\nu$  (i.e. the Prandtl number  $P_r = 1$ ), where  $g$  is the specific gravitational force, and  $a$  is the volume expansion coefficient. Substituting  $g \sim GM/R^2$ ,  $\nu = \alpha c_s H = \alpha c_s^2/\Omega_K$ , and  $\Omega_K^2 \sim GM/R^3$ , one has  $R_a \sim a\Delta T/(H/R)^4\alpha^2$ . Now  $a \sim 10^{-3} - 10^{-4}$  for gaseous materials, and  $\Delta T$  must be more than enough to make  $(a\Delta T)$  larger than unity, then for moderate values  $(H/R) \sim 0.1$  and  $\alpha \sim 0.01$ ,  $R_a$  safely exceeds 1000, the critical value required by laboratory convection. This argument further implies that convection is likely to develop in the radial direction of the flow.
4. In our solutions the very low efficiency of energy release  $\varepsilon$  corresponds to the net energy flux  $F$  that results from the competition of the advective, dissipative, and convective components. For a plain RIAF, i.e. that with zero radiative cooling,  $F$  flows constantly either

inward toward the central black hole ( $F < 0$ , type II solution) or outward toward the outer boundary of the flow ( $F > 0$ , type III solution). If a RIAF is not plain, i.e. a very small but non-zero amount of energy is radiated away, which is more likely to be the realistic case, then  $F$  provides energy available for radiation, and  $\varepsilon$  gives an estimation of the radiative efficiency. Certainly, this very small radiative loss of energy cannot affect the dynamics of the flow.

## ACKNOWLEDGMENTS

This work is supported by the National Science Foundation of China under Grant No.10233030.

## REFERENCES

Abramowicz M. A., Igumenshchev I. V., Quataert E., Narayan R., 2002, *ApJ*, 565, 1101  
 Balbus S. A., Hawley J. F., 1991, *ApJ*, 376, 214  
 Chen X., Abramowicz M. A., Lasota J.-P., 1997, *ApJ*, 476, 61  
 Hawley J. F., Balbus S. A., 2002, *ApJ*, 573, 738  
 Igumenshchev I. V., 2002, *ApJ*, 577, L31  
 Igumenshchev I. V., Abramowicz M. A., 1999, *MNRAS*, 303, 309  
 Igumenshchev I. V., Abramowicz M. A., 2000, *ApJS*, 130, 463  
 Igumenshchev I. V., Abramowicz M. A., 2001, in Wheeler J. C., Martel H., eds, The 20th Texas Symposium on Relativistic Astrophysics (astro-ph/0102482)  
 Igumenshchev I. V., Abramowicz M. A., Narayan R., 2000, *ApJ*, 537, L27  
 Igumenshchev I. V., Chen X., Abramowicz M. A., 1996, *MNRAS*, 278, 236  
 Lu J.-F., Gu W.-M., Yuan F., 1999, *ApJ*, 523, 340  
 Machida M., Matsumoto R., Mineshige S., 2001, *PASJ*, 53, L1  
 McKinney J. C., Gammie C. F., 2002, *ApJ*, 573, 728  
 Narayan R., 2002, in Gilfanov M., Sunyaev R., Churasov E., eds, Lighthouses of the Universe, Springer, New York (astro-ph/0201260)  
 Narayan R., Igumenshchev I. V., Abramowicz M. A., 2000, *ApJ*, 539, 798  
 Narayan R., Kato S., Honma F., 1997, *ApJ*, 476, 49  
 Narayan R., Mahadevan R., Quataert E., 1998, in Abramowicz M. A., Björnsson G., Pringle J. E., eds, The Theory of Black Hole Accretion Discs, Cambridge Univ. Press, Cambridge, 148  
 Narayan R., Yi I., 1994, *ApJ*, 428, L13  
 Narayan R., Yi I., 1995, *ApJ*, 452, 710  
 Paczyski B., Wiita P. J., 1980, *A&A*, 88, 23  
 Pen U.-L., Matzner C. D., Wong S., 2003, *ApJ*, 596, L207  
 Quataert E., Gruzinov A., 2000, *ApJ*, 539, 809  
 Stone J. M., Pringle J. E., Begelman M. C., 1999, *MNRAS*, 310, 1002